Molecular Pharmacology Fast Forward. Published on August 3, 2006 as doi:10.1124/mol.106.022194

Inhibition of in vivo glioma growth and invasion by PPARgamma agonist treatment

Christian Grommes, Gary E. Landreth, Magdalena Sastre, Martina Beck, Douglas L Feinstein, Andreas H. Jacobs, Uwe Schlegel, Michael T. Heneka

CG, GEL Department of Neurosciences, Alzheimer Research Laboratory, Case Western Reserve University, OH, USA

CG Department of Neurology, Case Western Reserve University, OH, USA

MTH Department of Neurology, University of Muenster, Germany

MS, MB Department of Neurology, University of Bonn Medical Center, Germany;

US Department of Neurology, University of Bochum, Bochum

DLF Department of Anesthesiology, University of Illinois, Chicago, Illinois, USA

AH Department of Neurology, University of Cologne, Germany

Molecular Pharmacology Fast Forward. Published on August 3, 2006 as DOI: 10.1124/mol.106.022194
This article has not been copyedited and formatted. The final version may differ from this version.

Running head title: Pioglitazone in glioma therapy

Corresponding author

Michael T. Heneka
Department of Neurology
University of Muenster
Albert-Schweitzer-Str. 33
48149 Muenster
Germany
Phone: +49 251 980 2810
Fax: +49-251 980 2804
Email: heneka@uni-muenster.de

Number of

Text pages:	22
Tables:	0
Figures:	5 (regular), 6 (suppl.)
References:	44

Number of words in

Abstract:	193
Introduction:	606
Discussion:	1261

Non-standard abbreviations used: retinoic acid receptor (RXR); PPAR-responsive elements (PPRE); pioglitazone (pio); 3-[4,5-dimethylthiazol-2-yl]-2,5-diphenyltetrazolium bromide (MTT); propidium iodide (PI).

Molecular Pharmacology Fast Forward. Published on August 3, 2006 as DOI: 10.1124/mol.106.022194
This article has not been copyedited and formatted. The final version may differ from this version.

Abstract:

The peroxisome proliferator-activated receptor gamma (PPARγ), a member of the nuclear hormone receptor family, represents a possible new target in glioma therapy. Since PPARγ plays a crucial role in regulation of insulin-sensitivity, synthetic agonists are already in clinical use for type II diabetes treatment. Beyond these metabolic effects, PPARγ agonists exhibit antineoplastic effects. Here, we investigated the antineoplastic effects of the PPARγ agonist pioglitazone in glioma cells. Pioglitazone reduced cellular viability of rat, human and PPARγ overexpressing glioma cells *in vitro* in a time- and concentration-dependent manner. No antineoplastic effects were induced by pioglitazone in glioma cells overexpressing a PPARγ mutant. Furthermore, proliferation was reduced by pioglitazone, measured by Ki-67 immunoreactivity, *in vitro*. Continuous intracerebral infusion of pioglitazone into gliomas induced by intrastriatal injection of C6 cells reduced tumor volumes by 83%. Oral administration of pioglitazone reduced tumor volumes by 76.9%. Subsequent brain tissue analysis revealed induction of apoptotic cell death. Ki-67-expression and BrdU-incorporation revealed a reduction of proliferation *in vivo*. Reduced invasion of C6 cells and lower MMP9 levels *in vivo* indicate pio-mediated reduction of invasion. Together, these data indicate that pioglitazone may be of potential use in treatment of malignant gliomas.

Molecular Pharmacology Fast Forward. Published on August 3, 2006 as DOI: 10.1124/mol.106.022194
This article has not been copyedited and formatted. The final version may differ from this version.

Introduction

Malignant astrocytic gliomas are the most common primary brain tumors. Glioma cells show a high proliferation rate and diffusely infiltrate adjacent brain tissue (Kleihues et al., 2002). These tumors initially respond to radiation and to a lesser degree to chemotherapy, however, they invariably recur. Despite substantial efforts, no curative therapy exists and the median overall-survival of the most malignant variant "glioblastoma" is poor (Nieder et al., 2005; Reardon et al., 2006; Stupp et al., 2005).

A new antineoplastic approach may lie in targeting the peroxisome proliferator-activated receptor γ (PPARγ) with specific agonists. PPARs are a subclass of nuclear hormone receptors, enabling the cell to respond to extracellular stimuli by transcriptionally regulating gene expression. Three isoforms of PPARs have been identified and designated as -α, -β/δ, and –γ and encoded by different genes. PPARs form heterodimers with the retinoic acid receptor (RXR) and exhibit ligand-induced transcriptional regulatory activity through sequence-specific PPAR-responsive elements (PPRE) in their target genes (Willson et al., 2000). For more than a decade work on PPARs was driven by their important role in the regulation of cellular metabolism, especially in tissues known for high rates of β-oxidation such as liver, heart, muscle and kidney. Since activation of the PPARγ subtype results in reduced serum glucose (Lemberger et al., 1996) recently developed synthetic PPARγ agonists are already in clinical use as anti-diabetic drugs (pioglitazone (ACTOS®); rosiglitazone (AVANDIA®)).

Apart from well defined metabolic actions, PPARγ agonists exhibit several antineoplastic effects (Grommes et al., 2004) and induce apoptotic cell death in various malignant cell lineages, including liposarcoma (Tontonoz et al., 1997), breast adenocarcinoma (Elstner

Molecular Pharmacology Fast Forward. Published on August 3, 2006 as DOI: 10.1124/mol.106.022194
This article has not been copyedited and formatted. The final version may differ from this version.

et al., 1998; Mueller et al., 1998), prostate carcinoma (Kubota et al., 1998), colorectal carcinoma (Brockman et al., 1998; Sarraf et al., 1998), non-small cell lung carcinoma (Chang and Szabo, 2000), pancreatic carcinoma (Motomura et al., 2000), bladder cancer (Guan et al., 1999), and gastric carcinoma (Sato et al., 2000). We recently reported that several PPARγ agonists induce apoptosis in rat and human glioma cell lines and a PPARγ antagonist and BAX antisense oligonucleotides blocked the apoptotic cell death induced by PPARγ-ligands (Grommes et al., 2005; Zander et al., 2002). Additionally, a recent study has shown PPARγ agonist mediated reduction of glioma cell survival caused by an increased production of reactive oxygen species (Perez-Ortiz et al., 2004). Furthermore, PPARγ agonists moderately inhibited growth of BT4Cn rat glioma cells, an effect which was abolished by the PPARγ antagonist GW9662 (Berge et al., 2001). A significant proportion of glioma tissues from 20 patients expressed PPARγ mRNA (Kato et al., 2002).

The present study demonstrates that the PPARγ agonist pioglitazone (pio) reduces cellular viability of C6 rat glioma and human glioma cell lines (A172, U87) and inhibits C6 glioma cell proliferation, measured by Ki-67 expression, *in vitro*. Furthermore, pioglitazone treatment in PPARγ-cDNA overexpressing glioma cells reduced cellular viability in glioma cells, while treatment of glioma cells overexpressing the PPARγ mutant E499Q-cDNA, which lacks the transcriptional activity, shows no antineoplastic effects. These findings were confirmed *in vivo* using a C6 rat glioma model. Here tumor volumes were reduced by 83% following intracerebral pio administration and by 76.9% with oral pio treatment. In parallel, pio treated animals exhibited improved clinical outcome, a lower proliferation-index (Ki-67) and decreased BrdU-incorporation within

Molecular Pharmacology Fast Forward. Published on August 3, 2006 as DOI: 10.1124/mol.106.022194
This article has not been copyedited and formatted. The final version may differ from this version.

the tumor tissue. In addition, in drug-treated animals tumors exhibited an upregulation of the proapoptotic proteins Bax and cleaved caspase-3 associated with increased TUNEL-labeling indicative of apoptotic cell death. Furthermore, reduced invasion measured *in vitro* with Boyden chamber experiments and *in vivo* through MMP9 levels, was observed. Pio also induced upregulation of the astrocytic redifferentiation marker CS-56 in tumor cells *in vitro* and *vivo,* a sign of induced redifferentiation.

Materials and Methods

Materials: Pioglitazone (Takeda Chemical Industries, Osaka, Japan) was dissolved in dimethyl sulfoxide (DMSO) obtained from Sigma (St. Louis, MO, USA). Dulbecco's modified Eagle's medium (DMEM), RPMI-1640 medium, penicillin, streptomycin, fetal calf serum, phosphate-buffered saline (PBS), trypsin-EDTA, and Proteinase K were purchased from Gibco (Gibco BRL, Karlsruhe, Germany). Rabbit Ki-67-antibody was purchased from NeoMarkers (Fremont, CA, USA), rabbit cleaved caspase-3- and rabbit BAX-antibody from Cell Signaling (Beverly, MA, USA), goat anti-MMP9 from Santa Cruz (Santa Cruz, CA, USA), and mouse anti-CS-56 from Sigma (St. Louis, MO, USA). For western blot analysis the secondary anti-rabbit-antibody was obtained from Amersham Bioscience (Piscataway, NJ, USA). Secondary antibody for immunohistochemistry (Alexa Fluor ® 488-conjugated goat anti-rabbit IgG) was purchased from Molecular Probes (Eugene, OR, USA).

Cell culture: Rat C6 glioma and murine cells were grown in DMEM and human glioma cells (U87, A172) in RPMI, supplemented with 10% (v/v) fetal calf serum, 100 U/mL penicillin and 100 U/mL streptomycin in a 5% CO_2 atmosphere. Primary astrocyte

Molecular Pharmacology Fast Forward. Published on August 3, 2006 as DOI: 10.1124/mol.106.022194
This article has not been copyedited and formatted. The final version may differ from this version.

cultures were prepared as previously described (McDonald et al., 1998) and grown in DMEM, supplemented with 2.5% (v/v) fetal calf serum, 100 U/mL penicillin and 100 U/mL streptomycin in a 5% CO_2 atmosphere.

Viability assay: Cellular viability was assessed by 3-[4,5-dimethylthiazol-2-yl]-2,5-diphenyltetrazolium bromide (MTT; Sigma, St. Louis, MO, USA) assay. Briefly, C6 cells, U87 cells and A172 cells ($5x10^3$/well) or primary astrocytes ($5x10^3$/well) were seeded in a 96-well plate and exposed to different concentrations of pio (1, 10, and 30 µM; n=10). DMSO served as vehicle control (0.1% of final concentration). At 1, 3, 5, and 7 days, 10 µl MTT (5 mg/ml PBS) was added to each well and plates were incubated at 37˚C for 2 h. Medium was then removed and cells were resuspended in 100 µl DMSO. Cell viability was assessed by colorimetric change using Spectramax 340PC plate reader (Molecular Devices, Sunnyvale, CA, USA) at λ=550nm. To ensure stability of pioglitazone at 37ºC, the compound was incubated over 21 day at 37ºC and cellular viability of C6 cells was assessed after 5 days. Experiments were performed in triplicate.

Transfection: Transfections were carried out on human A172 glioma cells using Lipofectamine 2000 (Invitrogen) according to the manufactur's instructions. PPARγ cDNA constructs were kindly provided by Dr. Ron Evans, The Salk Institute for Biological Studies, San Diego, USA (Mouse PPARgamma1 cDNA), from Dr. Evan Rosen, Harvard, USA (mouse PPARgamma2) from Dr. Bruce Spiegelman, Harvard, USA (mouse PPARgamma2 cDNA mutated at position E499Q31, a point mutation from Glu^{499} to Gln^{499} in the AF-2 activation domain, lacking its transcriptional activity). 48h

Molecular Pharmacology Fast Forward. Published on August 3, 2006 as DOI: 10.1124/mol.106.022194
This article has not been copyedited and formatted. The final version may differ from this version.

after transfection cells were treated with 30 μM pioglitazone. Cell viability was assessed after 5d using the above-described MTT assay. Experiments were performed in triplicates and repeated three times.

Animals: Spraque-Dawley rats (Charles River Laboratories, Sulzfeld, Germany) weighting 200-250 g and C57Bl/6 mice (Charles River Breeding, Cambridge, MA) age 6-8 weeks were used. Animals were housed in groups of two under standard conditions at a temperature of 22˚C±1 and a 12-h light-dark cycle with free access to food and water. Experiments were carried out in accordance with the declaration of Helsinki and were approved by the local ethical committee for animal experiments.

Brain tumor xenograft: Before implantation, 85–90% confluent C6 cells were trypsinized, rinsed with DMEM + 10% fetal calf serum, and centrifuged at 1000 rpm for 4 min. The cell pellet was resuspended in DMEM and placed on ice. Concentration of viable cells was adjusted to 1 x 10^5 cells/1 μl of DMEM. Each rat was anesthetized and placed in a stereotactic frame (David Kopf Instruments, Tujunga, CA, USA), a hole was drilled at AP 0.0, R –3.0 relative to bregma according to the stereotaxic atlas of König and Klippel (König and Klippel, 1963). Tumor cells were injected at a rate of o.5 μl/s, using a 2 μl Hamilton (#2701) syringe (Reno, NV, USA) with a 26s-gauge needle mounted on a stereotactic holder at a depth of 5 mm. The needle was left in place for a further 5 min to prevent reflux along the needle tract. For intracerebral administration of pio/vehicle (DMSO), the tip of an Alzet-brain-infusion-kit (Cupertino, CA, USA) was placed in a depth of 5 mm, connected to a 2ML4 Alzet osmotic pump (Cupertino, CA,

Molecular Pharmacology Fast Forward. Published on August 3, 2006 as DOI: 10.1124/mol.106.022194
This article has not been copyedited and formatted. The final version may differ from this version.

USA). Drug administration began 4 h after surgery. The osmotic pumps had a 2ml volume and 2.5µl/hour flow rate. The pumps were filled with 20µM pio solved in PBS or vehicle (DMSO, 0.1% final concentration) solved in PBS. Animals were randomly distributed in two groups, treated with pio filled pumps (n=26) or vehicle filled pumps (n=26). Thereafter skull was cleaned and the incision sutured. For oral treatment the drug was pulverized, and mixed with Purina chow to give concentrations of 120ppm pioglitazone. Control animals received Purina chow without additions. Rats were allowed free access to the chow. Tumors were allowed to grow and animals were weighed daily. The intracerebral treated animals were sacrificed after 3d (n=5/group), 6d (n=5/group), 9d (n=5/group), 14d (n=5/group), and 21d (n=6/group), the orally treated animals after 21d (n=8/group). C57Bl/6 mice (13 animals/group) received a single right frontal intracerebral injection of 5.0 X 10^4 cells of the murine glioma cell line GL261 and were treated with oral pioglitazone (100 ppm) mixed with mouse diet. Control animals received a single intracerebral injection of the equivalent number of GL261 cells without treatment.

Clinical assessment: After striatal injection of C6 cells and intracerebral treatment with pio or vehicle for 21d, the animals were examined for neurological deficits. Neurological function was quantified by evaluation of hemiparesis, cycling and immobility (Krajewski et al., 1986; Schabitz et al., 1999). Hemiparesis was assessed by forelimb flexion and immobility by the loss of ability to walk a distance greater than 15cm. One point was given for each negative finding and total score then computed. The scores of the treated and untreated group were averaged. A blinded observer performed neurological examinations.

Molecular Pharmacology Fast Forward. Published on August 3, 2006 as DOI: 10.1124/mol.106.022194
This article has not been copyedited and formatted. The final version may differ from this version.

Sections: Brains were serially sectioned at 10µm using a cryostat (Leica, Jung CM1800, Germany). Sections for hematoxylin-eosin (HE)-staining were placed onto uncoated slides. Sections intended for use in immunoreactivity assays were placed onto coated slides (Fisher finest, premium; Houston, TX, USA). Sections were routinely HE-stained for histomorphological assessment and measurement of tumor volume as well as immunohistochemically processed for Ki-67-, BAX, cleaved caspase-3- expression, MMP9, CS-56 and BrdU-incorporation.

Tumor volume: Images of HE-stained sections containing tumors were captured with a SPOT model 1.3 camera (Diagnostic Instruments, Inc., Sterling Heights, MI, USA) using a 1x objective and images processed using NIH Image 1.62 software (Bethesda, MD, USA). The tumor area of each section was manually outlined by a blinded observer using the freehand selection tool to measure tumor area in mm^2. The area was then multiplied by the section thickness (10µm section, 10 sections/HE stain) to achieve a section volume measurement. Volumes of all sections were added to calculate the total volume of each tumor. Tumor volumes for five/six animals of every group were measured.

Western-blot: For western-blot analysis, tumor-containing hemispheres were homogenized in Tris-HCl [50mM Tris-HCl pH8, 120mM NaCl, 5mM EDTA, 0.5% (v/v) NP-40, 160mM phenylmethylsulfonyl fluoride (PMSF)] and sonicated. Homogenates were collected by centrifugation (15 min, 11000*g,* 4°C) and protein concentration of the

Molecular Pharmacology Fast Forward. Published on August 3, 2006 as DOI: 10.1124/mol.106.022194
This article has not been copyedited and formatted. The final version may differ from this version.

supernatant was determined using the Bio-Rad Protein Assay (Biorad, Munich, Germany). Lysates (20-40µg) were separated on a 7% (w/v) sodium dodecyl sulfate (SDS)-polyacrylamide gel under reducing conditions and transferred to a PVDF membrane (Millipore, Bedford, MA, USA). Non-specific binding was blocked by incubation with 5% (w/v) skimmed milk in TBS for 2h. Following incubation with the primary antibody overnight at 4˚C [rabbit anti-BAX 1:1000, rabbit anti-cleaved caspase-3 1:1000, mouse anti-CS-65 1:1000, goat anti-MMP-9 1:1000 in TBS containing 0.1% (v/v) Tween 20] membranes were washed three times in TBS/Tween for 5 min and subsequently incubated for 120 min in TBS/Tween containing secondary peroxidase-conjugated antibody at room temperature (anti-rabbit 1:1000, anti-mouse 1:1000; anti-goat 1:1000 respectively). Signals were visualized by chemoluminescence (Pierce, Rockford, IL, USA) and band intensities were quantified with NIH Image 1.62 software (Bethesda, MD, USA).

Immunohistochemistry: Frozen brain sections were first blocked with 5% normal goat serum or normal horse serum in PBS and subsequently incubated with rabbit anti-Ki-67 antibody (1:200 dilution), mouse anti-CS-56 (1:100 dilution), goat anti-MMP-9 (1:100 dilution) or rabbit anti-cleaved caspase-3 antibody (1:200 dilution) at 4˚C overnight. Sections were washed extensively with PBS before incubation with secondary antibodies. Incubation was carried at room temperature for 1 h. After washing with PBS three times, stained slides were mounted with PBS/ glycerol (1:1) and viewed under a fluorescent microscope (Leica, Germany).

C6 glioma cell cultures were treated with pio or vehicle for 2d and 5d and fixed in 4% paraformaldehyde, rinsed in TBS and incubated with rabbit anti-Ki-67 (1:200 dilution) at

Molecular Pharmacology Fast Forward. Published on August 3, 2006 as DOI: 10.1124/mol.106.022194
This article has not been copyedited and formatted. The final version may differ from this version.

4˚C overnight and processed as described above. Counterstaining was carried out with propidium iodide (PI; 1:40; Sigma, St. Louis, MO, USA) or DAPI-staining (1:500 in PBS). For determination of the proliferation-index, Ki-67 positive cells in pio and vehicle treated cells and animals were counted, the percentage of Ki-67 positive cells in $1x10^3$ tumor cells (PI staining used in the *in vitro* experiments - not shown; DAPI stain used in the *in vivo* experiments) calculated and statistically compared. The percentage of cleaved caspase-3 positive cells was assessed by counting the immunopositive cells in $1x10^3$ tumor (DAPI stain) cells and statistically compared. Negative controls showed no immunreactivity.

Terminal Deoxynucleotidyl Transferase-Mediated dUTP Nick-End Labeling Assay for Apoptosis: Frozen brain tissue sections were examined for apoptosis using the terminal deoxynucleotidyl transferase-mediated dUTP transferase nick-end labeling (TUNEL assay). Apoptosis was evaluated using the Promega DeadEnd Fluorometric Tunel System (Promega, Madison, WI, USA) according to the manufacturer's instructions. The percentage of TUNEL positive cells was assessed by counting the immunopositve cells in $1x10^3$ tumor (DAPI stain) cells and statistically compared.

BrdU incorporation: At thirteen days of treatment animals were intraperitoneally injected with 300 mg/kg of 5-bromodeoxyuridine (BrdU; Sigma, St. Louis, MO), a thymidine analog that incorporates into the DNA of dividing cells during S phase and can be detected immunohistochemically. Twenty-four hours later, these animals were anesthetized and perfused with phosphate-buffered saline (PBS). Brains were dissected, frozen, cut and immunostained in the following manner: Sections were fixed

Molecular Pharmacology Fast Forward. Published on August 3, 2006 as DOI: 10.1124/mol.106.022194
This article has not been copyedited and formatted. The final version may differ from this version.

in 4% paraformaldehyde, washed in PBS, and incubated in 2 N HCl for 10 min at room temperature. Sections were again washed in PBS and incubated in BrdU primary antibody (rat monoclonal 1:100, Abcam, Cambridge, UK) in PBS containing 5% normal goat serum overnight at 4˚C. After washing with PBS, sections were incubated in rhodamine-labeled anti-rat secondary antibody (1:100, Jackson, West Grove, PA, USA) in PBS containing 5% normal goat serum for 1 h at room temperature. The number of dividing cells present in the tumor of these BrdU-stained sections was then counted and compared to total amount of tumor cells stained with DAPI.

Boyden-Chamber-assay:

C6 cell migration in the presence or absence of pio was assessed using a Boyden chamber (AP48, NeuroProbe, Gaithersburg, MD, USA) with an 8 µm polycarbonate PVPF-filter (Osmonics, Minnetonka, MN, USA). Cells were suspended in DMEM containing 2.5% fetal calf serum and pio at 30µM or vehicle (DMSO). C6 glioma cells were pretreated for 24h in the presence or absence of 30µM pio. Cells ($5x10^3$ in 50µl pio/medium or vehicle/medium) were then plated in the wells of the upper compartment of the chamber (6 wells/condition), and the wells of the lower compartment were filled with DMEM. Incubation was performed at 37°C in 5% CO_2 for 4 h. After incubation, cells on the upper surface of the filter, which had not migrated, were gently scraped off, and the filters were then fixed in methanol and subsequently stained with DAPI (1:500 in PBS; Sigma, St. Louis, MO, USA). Cells which had migrated to the lower surface of the filters, were counted using public domain software NIH Image 1.62 (Bethesda, MD, USA). The total numbers of migrating cells under pio treated and vehicle treated conditions were compared statistically. Experiments were performed in duplicate.

Molecular Pharmacology Fast Forward. Published on August 3, 2006 as DOI: 10.1124/mol.106.022194
This article has not been copyedited and formatted. The final version may differ from this version.

Statiatical evaluation: Cellular viability data, tumor volumes, immuno-positive cells, clinical scores, proliferation-index and densitometric results of Bax and cleaved caspase-3 western-blots were analyzed by student-T-test using Prism version 3.00 software (GraphPad Software, San Diego, CA, USA).

Results

Reduced cellular viability of rat C6 glioma and human glioma cells: Viability of rat C6 glioma cells and human glioma cells (U87, A172) was assessed after incubation with increasing concentrations (1, 10, 30 µM) of the PPARγ agonist pio at day 1, 3, 5, and 7 (Fig. 1A, B). Ten and 30 µM pio significantly reduced the cellular viability of C6 rat glioma cells in a concentration- and time-dependent manner (Fig. 1A). A significant reduction of cellular viability in C6 cells was observed at 5 d and 7 d after treatment with 30 µM pio and at 7 d after treatment with 10 µM pio (Fig. 1A). At 7 d, 30 µM of pio reduced viability to 31% ± 3.7, and 10µM of pio to 52.1% ± 6.4 (Fig. 1A). In the human glioma cell lines U87 and A172, 10 and 30 µM pio significantly reduced cellular viability at 3, 5, and 7 d (Fig. 1B, supplement Fig. 4).

At all time points and concentrations evaluated, viability of primary astrocytes was not affected by pio treatment (Fig. 1C), indicating that PPARγ ligand-mediated cell death is restricted to neoplastic astrocytic cells.

To assess the role of PPARγ in the antineoplastic effects of pio, we overexpressed PPARγ in the human glioma cell line A172. Pio treatment and overexpression of two different PPARγ-cDNA, PPAR1 and 2, reduced cellular viability of A172 cells measured

Molecular Pharmacology Fast Forward. Published on August 3, 2006 as DOI: 10.1124/mol.106.022194
This article has not been copyedited and formatted. The final version may differ from this version.

by MTT compared to medium and vector controls. After transfection of A172 cells with a PPARγ mutant-cDNA lacking transcriptional activity the decrease in effects on cellular viability were no longer observed at 5d following transfection (Fig 1D).

Ki-67 immunoreactivity and proliferation-index is reduced after pioglitazone treatment *in vitro*: To further characterize the pio-induced effects, Ki-67 expression, a marker for tumor proliferation and malignancy, was evaluated. C6 cells were treated with 30 µM pio or vehicle and Ki-67 immunoreactivity was assessed at 2d (supplement Fig 1A, B) and 5d (supplement Fig 1C, D). Pio reduced the number of Ki-67 immunopositive cells compared to vehicle treatment at both time points. Thus, the fraction of Ki-67 positive, proliferating cells, expressed as proliferation-index, was significantly reduced after 5 d of pio treatment (supplement Fig. 1E).

Significantly reduced tumor volume and growth in the rat glioma model: In order to confirm the antineoplastic effects of pio *in vivo*, C6 glioma cells were injected in rat striata and treated with pio 20 µM or vehicle via an osmotic pump for 3d (n=5/group), 6d (n=5/group), 9d (n=5/group), 14d (n=5/group), or 21d (n=6/group) starting 4h after initial tumor cell injection. *In vitro* studies demonstrated that the biological activity of pioglitazone remains stable when incubated at 37ºC over 21 days (reduction of cellular viability to 31%±3.7 prior to incubation and 31.7%±7.4 after incubation; supplemental Figure 6).

The pio-treated animals showed a dramatic reduction of tumor volume at 21 days of treatment (Fig. 2B, D, E) compared to vehicle-treated animals (Fig. 2A, C, E). Vehicle-

Molecular Pharmacology Fast Forward. Published on August 3, 2006 as DOI: 10.1124/mol.106.022194
This article has not been copyedited and formatted. The final version may differ from this version.

treated animals exhibit a median tumor volume of 0.321cm^3 ± 0.11 whereas pio-treated animals revealed tumor volumes of 0.055cm^3 ± 0.03, reflecting an 83% reduction (Fig.2G). At 3 and 6 days no significant differences in tumor volumes could be observed (Fig. 2F). However, at 9, 14, and 21 days tumor volumes decreased significantly in pio treated animals (Fig. 2F). These effects were also observed in the oral treated animals, where pio treatment reduced tumor volumes by 76.9% after 21 days (Fig. 2H).

Similar results were observed in a mouse model as well. C57Bl/6 mice (13 animals/group) received a single right frontal intracerebral injection of the murine glioma cell line GL261 and were treated with oral pioglitazone (100 ppm) mixed with mouse diet. Control animals received a single intracerebral injection of the equivalent number of GL261 cells without treatment. At day 30 the number of surviving animals was 3.6 fold higher in the pio treated group (supplemental Fig. 5)

Improved clinical outcome: To investigate whether the reduction of tumor volumes results in improved neurological outcome, animals were assessed and scored for signs of hemiparesis, cycling and immobility as previously described (Krajewski et al., 1986; Schabitz et al., 1999). Pio-treated animals had a significantly better clinical outcome overall. They exhibited less hemiparesis, no cycling, and less immobility (supplement Fig. 2) then vehicle treated control animals.

Animals were also closely monitored for weight-loss, a non-behavioral indicator of intracellular tumor growth (Redgate et al., 1991). Daily weighing of animals showed the vehicle-treated group exhibiting a significant weight loss at 17 days, whereas pio-treated animals did not show any weight loss (supplement Fig. 2E). Together, these clinical

Molecular Pharmacology Fast Forward. Published on August 3, 2006 as DOI: 10.1124/mol.106.022194
This article has not been copyedited and formatted. The final version may differ from this version.

evaluations suggest that pio-induced reduction of tumor volume improved clinical outcome.

Induction of apoptotic cell death *in vivo*: To assess if pio induces apoptotic cell death *in vivo* Bax- and cleaved caspase-3-expression were evaluated and TUNEL staining was performed. The expression of the proapoptotic proteins Bax and cleaved caspase-3 was detected in whole-hemisphere lysates of C6 glioma animals and controls. Analysis at different time points revealed that both proteins were expressed in the pio treated animals and in controls (Fig. 3A). Protein levels of either Bax or cleaved caspase-3 were upregulated in the early phase of pio treatment. Densitometric analysis showed a significant difference in Bax-protein levels at 3, 6, 9, and 14 days (Fig. 3D) and in cleaved caspase-3-protein levels at 3, 6, and 9 days (Fig. 3E) in response to pio treatment. At 6 days of pio treatment Bax and cleaved caspase-3 were upregulated (Fig. 3B) with a 4.49 fold induction of Bax protein (Fig. 3D) and a 3.83 fold induction of cleaved caspase-3 (Fig. 3E).

Immunohistochemistry revealed elevated cleaved caspase-3 expression at 6 to 14 days of pio treatment with a significant maximum at 9 days (Fig. 4B) compared to vehicle treated animals (Fig. 4A). DAPI staining was used to tag single tumor cells and to determine the percentage of cleaved caspase-3 positive cells (Fig. 4C). Increased TUNEL staining was detected at 9 days of pio treatment (Fig. 4E). Very few cells were positively TUNEL stained in vehicle controls (Fig. 4D).

Ki-67 immunoreactivity and proliferation-index is reduced *in vivo*: Ki-67 expression was used to evaluate degree of tumor proliferation *in vivo*. C6 glioma animals showed

Molecular Pharmacology Fast Forward. Published on August 3, 2006 as DOI: 10.1124/mol.106.022194
This article has not been copyedited and formatted. The final version may differ from this version.

significant reduction of Ki-67 expression at 9, 14, and 21 days of pio treatment (Fig. 4H) compared to vehicle-treated animals (Fig. 4G). The proliferation-index, calculated from the percentage of Ki-67 positive cells in $1x10^3$ tumor cells (DAPI), was reduced by pio treatment at 9, 14 and 21 days (Fig. 4I) confirming the results obtained *in vitro*.

Reduction of BrdU-incorporation: To further confirm that pio treatment reduces proliferation, we assessed BrdU-incorporation *in vivo*. BrdU-incorporation was reduced in response to pio treatment at 14d (Fig. 4L) compared to the vehicle treated groups (Fig. 4K). The percentage of BrdU positive cells is significantly lower in pio treated animals (Fig. 4M).

Invasion of C6 rat glioma cells after pioglitazone treatment *in vitro*: In addition to proliferation, the ability of tumor cells to invade healthy near-by tissue is characteristic of the malignancy state of gliomas. Histological evaluation of pio treated *in vivo* gliomas revealed more defined tumor margins and decreased invasiveness (Fig. 2C,D). This led us to examine invasiveness of C6 glioma cells using a Boyden chamber assay. Pio-pretreated (30 µM) (supplement Fig. 3D, E, F) and untreated (supplement Fig. 3A, B, C) C6 glioma cells were suspended in the upper chamber containing pio at 30 µM (supplement Fig. 3B, E) or vehicle (supplement Fig. 3A, D). At 4h, cells that migrated to the other side of an 8 µm filter were stained with DAPI and counted. Pio treatment during the Boyden chamber incubation reduced the invasiveness of C6 cells significantly (supplement Fig. 3A, B, C). Pretreatment of C6 cells for 24h with pio further increased inhibition (supplement Fig. 3D, E, F).

Molecular Pharmacology Fast Forward. Published on August 3, 2006 as DOI: 10.1124/mol.106.022194
This article has not been copyedited and formatted. The final version may differ from this version.

MMP9 and CS-56 expression in vivo: In order to characterize the invasion of pio-treated tumors in vivo, we investigated levels of MMP-9, a protein which plays a major role in glioma invasion (Rao et al., 1993). MMP-9 expression was detected in whole-hemisphere lysates of C6 glioma animals using a goat-anti-MMP-9-antibody. MMP-9 expression was almost completely suppressed in pio-treated animals (Fig. 5A). Erk2 expression served as a loading control (Fig. 5A). Densitometric analysis showed an 81% reduction of MMP-9 expression in the pio-treated group (Fig. 5B). Immunoreactivity of MMP-9 revealed that the epitope is only expressed in the tumor and adjacent brain regions (Fig 5C). Pio treatment reduced MMP-9 positive staining at tumor margins and even more so in the surrounding healthy brain tissue compared to vehicle treatment (Fig.5C).

The expression of a marker of astrocytic differentiation, CS-56 (Vitellaro-Zuccarello et al., 2001), was evaluated in the tumors (Fig. 5C). An upregulation of CS-56 was most prominently observed at the tumor margin towards healthy brain tissue compared to vehicle-treated animals (Fig. 5C). Parallel analysis of tissue lysates by western-blot (Fig 5D) revealed upregulation of CS-56 expression in pio-treated animals, which was corroborated by the densitometrical measurement, showing an increase of around 56% inCS-56 protein levels (Fig. 5E). Erk2 expression served as a loading control (Fig 5D).

Discussion

Antineoplastic effects of PPARγ agonists on human tumor cells (Grommes et al., 2005) and rat glioma cell lines (Grommes et al., 2005; Zander et al., 2002) led us to question if the synthetic PPARγ agonist pioglitazone (pio) could exert similar effects in rat and

Molecular Pharmacology Fast Forward. Published on August 3, 2006 as DOI: 10.1124/mol.106.022194
This article has not been copyedited and formatted. The final version may differ from this version.

human glioma cells as well as in animal glioma models. Pio, a member of the thiazolidinedione (TZD) class of antidiabetic drugs, was chosen since it is already in clinical use for treatment of type II diabetes mellitus (ACTOS®) and would be readily available for glioma therapy in clinical studies. In the present study pio demonstrated antineoplastic potency *in vitro* by decreasing cellular viability of human and rat glioma cells. Similar effects were found in PPARγ overexpressing glioma cells, whereas pio treatment of glioma cells overexpressing a PPARγ-mutant, lacking the transcriptional activation, did not induce antineoplastic changes. We demonstrated that the reduction of cellular viability by pio is restricted to neoplastic cell types, as primary astrocytes were not affected by pio treatment. In our hand and in prior studies (Cullingford et al. 1998) normal rat astrocytes express PPAR gamma at low levels. We have previously shown that primary rat astrocytes are not susceptible to PPARgamma agonist induced cell death (Zander et al. 2002). This is contrary to the apoptotic cell death observed in human fetal astrocytes following treatment with PPARgamma agonists and may be due to species differences (Chattopadhyay et al. 2000).

Of the three glioma cell lines we studied, PPARγ protein levels are highest in U87 compared to A176 and C6 (Zander et al., 2002). Pio reduced cellular viability in human glioma cell line U87 more robustly than either A172 or C6 glioma cell lines, which may be related to the relative PPARγ protein levels expressed in these glioma cell lines.

Ki-67 is a nuclear protein expressed in proliferating cells and serves as an important neuropathological marker of human gliomas (Torp, 2002). In astrocytomas, Ki-67 expression is upregulated and correlates well with tumor grade and clinical prognosis (Brown and Gatter, 2002; Parkins et al., 1991). Pio treatment reduced Ki-67 expression

Molecular Pharmacology Fast Forward. Published on August 3, 2006 as DOI: 10.1124/mol.106.022194
This article has not been copyedited and formatted. The final version may differ from this version.

in vitro. Therefore, pio reduces both cellular viability and proliferation, leading to a reduced tumor cell number *in vitro*.

To verify these results *in vivo*, C6 cells were injected into rat striata (Stander et al., 1998) and either continuously treated with pio through an intracerebrally placed osmotic pump or orally for three weeks. Intracerebral pio treatment reduced tumor volumes by 83%, oral pio treatment by 76.9%. Furthermore, preservation of neurological function and body weight was observed in the pio-treated animals. Tumor volumes showed no significant difference during the early treatment period (3 and 6 days) indicating that pio treatment did not affect initial tumor inoculation. At 9 days tumor volumes increased in the vehicle group and decreased in the pio treated animals, indicating that antineoplastic effects of pio appear between days 6 to 9 *in vivo*, a time frame identical to our *in vitro* results. Similar antineoplastic effects of pio were seen in a murine animal model.

We investigated Bax protein expression because initial *in vitro* data indicate that PPARγ-agonists mediate their antineoplastic effects in rat and human glioma cell lines through a Bax upregulation leading to apoptosis, which could be abolished by Bax antisense-oligonucleotides (Zander et al., 2002). Primary data revealed that tumor growth reduction by pio was not associated with an upregulation of proapoptotic proteins after 21 days of treatment (data not shown), therefore earlier time points were evaluated. Bax as well as its downstream target cleaved caspase-3 peaked in the early phase of the treatment. At 6 days of pio therapy a significant induction of these proapoptotic proteins was observed, correlating with an increase in cleaved caspase-3 immunoreactivity and TUNEL labeling at day 9. In prior studies, we were able to demonstrate that the PPARgamma agonist induced apoptotic death is BAX-dependent (Zander et al. 2002).

Molecular Pharmacology Fast Forward. Published on August 3, 2006 as DOI: 10.1124/mol.106.022194
This article has not been copyedited and formatted. The final version may differ from this version.

Together, these findings indicate, that pio induced apoptosis of rat C6 gliomas occurred from days 6 to 9 and contributed at least in part to the observed reduction in tumor volume.

Reduced tumor growth might also be due to decreased proliferation, as observed *in vitro*. To assess if pio also reduces proliferation *in vivo* Ki67-expression and BrdU-incorporation was determined since earlier studies showed the ability of PPARγ agonists to reduce BrdU-incorportion in various cell lines (Fajas et al., 2003). Both proliferation markers were reduced by pio, indicating that pio not only induced apoptosis but also reduced proliferation.

Histological differences, better defined tumor margins and fewer invasive cells, following pio treatment led us to investigate pio-induced changes of invasion *in vitro* using the Boyden chamber assay, a reliable test for assessment of C6 cell migration and invasion (Sottocornola et al., 1998). Pio treatment resulted in dramatic reduction of cell migration. Furthermore, matrix-metalloproteinases (MMP) play a critical role in tumor invasiveness and in the malignancy of gliomas (Rao et al., 1993) by mediating basal membrane breakdown. MMP-9, the most abundant MMP in gliomas (Forsyth et al., 1999), is elevated during tumor progression (Rao et al., 1993) due to its secretion by glioma cells (Choe et al., 2002). Tumor growth and formation is blocked by MMP-9 antisense oligonucleotides *in vivo* (Lakka et al., 2002). In the present study, MMP-9 expression was dramatically reduced by 81% in pio-treated animals, particularly at the tumor margin. MMP-9 downregulation at the tumor margin may account for the reduced capability of pio-treated tumors to invade brain tissue. Whole brain slides were used for protein level evaluation through western blot. Therefore the ratio of MMP9 protein levels

Molecular Pharmacology Fast Forward. Published on August 3, 2006 as DOI: 10.1124/mol.106.022194
This article has not been copyedited and formatted. The final version may differ from this version.

in the tumor to brain tissue is smaller in the treated animals and could account for the lower MMP-9 signal detected by western blot when compared to the immunohistochemical stain.

Treatment of C6 cells with the PPARγ agonist ciglitazone lead to increased redifferentiation in prior studies (Zander et al., 2002). Therefore, we investigated protein levels and immunohistochemical localization of CS-56, an astrocytic redifferentiation marker. CS-56 expression reflects levels of chondroitin sulfate proteoglycans, the most abundant component of the extracellular matrix of mammalian brain (Herndon and Lander, 1990) which is involved in development and redifferentiation (Vitellaro-Zuccarello et al., 2001). CS-56 is located predominantly at the tumor border, where it is highly upregulated by pio treatment both *in vitro* (data not shown) and *in vivo*. Pio may therefore not only induce cell death and inhibition of proliferation in neoplastic cells but may also elicit redifferentiation in the malignant cells. The CS-56 upregulation at the tumor margin could also reflect glia formation separating tumor tissue from healthy brain tissue because CS-56 is strongly upregulated in glial scars (Davies et al., 1997).

The concentration of pio required to affect cellular viability is higher than expected according to its known *in vitro* receptor binding affinity (Sakamoto et al., 2000). PPARγ independent mechanisms have also been reported for thiazolidinediones (Chawla et al., 2001) and need to be considered. Troglitazone inhibits cholesterol biosynthesis (Wang et al., 1999) or acyl-CoA synthetase in a PPARγ-independent way (Kim et al., 2001). Pio treatment of human glioma cells overexpressing the PPARγ mutant E499Q, lacking the transcriptional activation, did not lead to a reduction of cellular viability, indicating that the described pio effects are indeed displayed in a PPARγ dependant way.

Molecular Pharmacology Fast Forward. Published on August 3, 2006 as DOI: 10.1124/mol.106.022194
This article has not been copyedited and formatted. The final version may differ from this version.

Although the molecular basis of antineoplastic mechanisms of PPARγ agonists are yet not fully understood, the thiazolidinediones may offer a new therapeutic approach in human glioma therapy due to their negative effects on proliferation and invasion as well as their positive effects on apoptosis and redifferentiation. However, further studies will be required to ascertain optimal mode and timing for application of pio.

References

Berge K, Tronstad KJ, Flindt EN, Rasmussen TH, Madsen L, Kristiansen K and Berge RK (2001) Tetradecylthioacetic acid inhibits growth of rat glioma cells ex vivo and in vivo via PPAR-dependent and PPAR-independent pathways. *Carcinogenesis* **22**:1747-55.

Brockman JA, Gupta RA and Dubois RN (1998) Activation of PPARgamma leads to inhibition of anchorage-independent growth of human colorectal cancer cells. *Gastroenterology* **115**:1049-55.

Brown DC and Gatter KC (2002) Ki67 protein: the immaculate deception? *Histopathology* **40**:2-11.

Chang TH and Szabo E (2000) Induction of differentiation and apoptosis by ligands of peroxisome proliferator-activated receptor gamma in non-small cell lung cancer. *Cancer Res* **60**:1129-38.

Chawla A, Barak Y, Nagy L, Liao D, Tontonoz P and Evans RM (2001) PPAR-gamma dependent and independent effects on macrophage-gene expression in lipid metabolism and inflammation. *Nat Med* **7**:48-52.

Choe G, Park JK, Jouben-Steele L, Kremen TJ, Liau LM, Vinters HV, Cloughesy TF and Mischel PS (2002) Active matrix metalloproteinase 9 expression is associated with primary glioblastoma subtype. *Clin Cancer Res* **8**:2894-901.

Davies SJ, Fitch MT, Memberg SP, Hall AK, Raisman G and Silver J (1997) Regeneration of adult axons in white matter tracts of the central nervous system. *Nature* **390**:680-3.

Elstner E, Muller C, Koshizuka K, Williamson EA, Park D, Asou H, Shintaku P, Said JW, Heber D and Koeffler HP (1998) Ligands for peroxisome proliferator-activated

receptorgamma and retinoic acid receptor inhibit growth and induce apoptosis of human breast cancer cells in vitro and in BNX mice. *Proc Natl Acad Sci U S A* **95**:8806-11.

Fajas L, Egler V, Reiter R, Miard S, Lefebvre AM and Auwerx J (2003) PPARgamma controls cell proliferation and apoptosis in an RB-dependent manner. *Oncogene* **22**:4186-93.

Forsyth PA, Wong H, Laing TD, Rewcastle NB, Morris DG, Muzik H, Leco KJ, Johnston RN, Brasher PM, Sutherland G and Edwards DR (1999) Gelatinase-A (MMP-2), gelatinase-B (MMP-9) and membrane type matrix metalloproteinase-1 (MT1-MMP) are involved in different aspects of the pathophysiology of malignant gliomas. *Br J Cancer* **79**:1828-35.

Grommes C, Landreth GE and Heneka MT (2004) Antineoplastic effects of peroxisome proliferator-activated receptor gamma agonists. *Lancet Oncol* **5**:419-29.

Grommes C, Landreth GE, Schlegel U and Heneka MT (2005) The non-thiazolidinedione tyrosine-based PPAR{gamma} ligand GW7845 induces apoptosis and limits migration and invasion of rat and human glioma cells. *J Pharmacol Exp Ther*.

Guan YF, Zhang YH, Breyer RM, Davis L and Breyer MD (1999) Expression of peroxisome proliferator-activated receptor gamma (PPARgamma) in human transitional bladder cancer and its role in inducing cell death. *Neoplasia* **1**:330-9.

Herndon ME and Lander AD (1990) A diverse set of developmentally regulated proteoglycans is expressed in the rat central nervous system. *Neuron* **4**:949-61.

Kato M, Nagaya T, Fujieda M, Saito K, Yoshida J and Seo H (2002) Expression of PPARgamma and its ligand-dependent growth inhibition in human brain tumor cell lines. *Jpn J Cancer Res* **93**:660-6.

Kim YS, Han CY, Kim SW, Kim JH, Lee SK, Jung DJ, Park SY, Kang H, Choi HS, Lee JW and Pak YK (2001) The orphan nuclear receptor small heterodimer partner as a novel coregulator of nuclear factor-kappa b in oxidized low density lipoprotein-treated macrophage cell line RAW 264.7. *J Biol Chem* **276**:33736-40.

Kleihues P, Louis DN, Scheithauer BW, Rorke LB, Reifenberger G, Burger PC and Cavenee WK (2002) The WHO classification of tumors of the nervous system. *J Neuropathol Exp Neurol* **61**:215-25; discussion 226-9.

König JFR and Klippel RA (1963) *The Rat Brain: A Stereotaxic Atlas of the Forebrain and Lower Parts of the Brainstem.* Williams and Wilkins, Baltimore, USA.

Krajewski S, Kiwit JC and Wechsler W (1986) RG2 glioma growth in rat cerebellum after subdural implantation. *J Neurosurg* **65**:222-9.

Kubota T, Koshizuka K, Williamson EA, Asou H, Said JW, Holden S, Miyoshi I and Koeffler HP (1998) Ligand for peroxisome proliferator-activated receptor gamma (troglitazone) has potent antitumor effect against human prostate cancer both in vitro and in vivo. *Cancer Res* **58**:3344-52.

Lakka SS, Rajan M, Gondi C, Yanamandra N, Chandrasekar N, Jasti SL, Adachi Y, Siddique K, Gujrati M, Olivero W, Dinh DH, Kouraklis G, Kyritsis AP and Rao JS (2002) Adenovirus-mediated expression of antisense MMP-9 in glioma cells inhibits tumor growth and invasion. *Oncogene* **21**:8011-9.

Lemberger T, Desvergne B and Wahli W (1996) Peroxisome proliferator-activated receptors: a nuclear receptor signaling pathway in lipid physiology. *Annu Rev Cell Dev Biol* **12**:335-63.

McDonald DR, Bamberger ME, Combs CK and Landreth GE (1998) beta-Amyloid fibrils activate parallel mitogen-activated protein kinase pathways in microglia and THP1 monocytes. *J Neurosci* **18**:4451-60.

Motomura W, Okumura T, Takahashi N, Obara T and Kohgo Y (2000) Activation of peroxisome proliferator-activated receptor gamma by troglitazone inhibits cell growth through the increase of p27KiP1 in human. Pancreatic carcinoma cells. *Cancer Res* **60**:5558-64.

Mueller E, Sarraf P, Tontonoz P, Evans RM, Martin KJ, Zhang M, Fletcher C, Singer S and Spiegelman BM (1998) Terminal differentiation of human breast cancer through PPAR gamma. *Mol Cell* **1**:465-70.

Nieder C, Grosu AL, Astner S and Molls M (2005) Treatment of unresectable glioblastoma multiforme. *Anticancer Res* **25**:4605-10.

Parkins CS, Darling JL, Gill SS, Revesz T and Thomas DG (1991) Cell proliferation in serial biopsies through human malignant brain tumours: measurement using Ki67 antibody labelling. *Br J Neurosurg* **5**:289-98.

Perez-Ortiz JM, Tranque P, Vaquero CF, Domingo B, Molina F, Calvo S, Jordan J, Cena V and Llopis J (2004) Glitazones differentially regulate primary astrocyte and glioma cell survival. Involvement of reactive oxygen species and peroxisome proliferator-activated receptor-gamma. *J Biol Chem* **279**:8976-85.

Rao JS, Steck PA, Mohanam S, Stetler-Stevenson WG, Liotta LA and Sawaya R (1993) Elevated levels of M(r) 92,000 type IV collagenase in human brain tumors. *Cancer Res* **53**:2208-11.

Reardon DA, Rich JN, Friedman HS and Bigner DD (2006) Recent advances in the treatment of malignant astrocytoma. *J Clin Oncol* **24**:1253-65.

Redgate ES, Deutsch M and Boggs SS (1991) Time of death of CNS tumor-bearing rats can be reliably predicted by body weight-loss patterns. *Lab Anim Sci* **41**:269-73.

Sakamoto J, Kimura H, Moriyama S, Odaka H, Momose Y, Sugiyama Y and Sawada H (2000) Activation of human peroxisome proliferator-activated receptor (PPAR) subtypes by pioglitazone. *Biochem Biophys Res Commun* **278**:704-11.

Sarraf P, Mueller E, Jones D, King FJ, DeAngelo DJ, Partridge JB, Holden SA, Chen LB, Singer S, Fletcher C and Spiegelman BM (1998) Differentiation and reversal of malignant changes in colon cancer through PPARgamma. *Nat Med* **4**:1046-52.

Sato H, Ishihara S, Kawashima K, Moriyama N, Suetsugu H, Kazumori H, Okuyama T, Rumi MA, Fukuda R, Nagasue N and Kinoshita Y (2000) Expression of peroxisome proliferator-activated receptor (PPAR)gamma in gastric cancer and inhibitory effects of PPARgamma agonists. *Br J Cancer* **83**:1394-400.

Schabitz WR, Li F, Irie K, Sandage BW, Jr., Locke KW and Fisher M (1999) Synergistic effects of a combination of low-dose basic fibroblast growth factor and citicoline after temporary experimental focal ischemia. *Stroke* **30**:427-31; discussion 431-2.

Sottocornola E, Colombo I, Vergani V, Taraboletti G and Berra B (1998) Increased tumorigenicity and invasiveness of C6 rat glioma cells transfected with the human alpha-2,8 sialyltransferase cDNA. *Invasion Metastasis* **18**:142-54.

Stander M, Naumann U, Dumitrescu L, Heneka M, Loschmann P, Gulbins E, Dichgans J and Weller M (1998) Decorin gene transfer-mediated suppression of TGF-beta synthesis abrogates experimental malignant glioma growth in vivo. *Gene Ther* **5**:1187-94.

Stupp R, Mason WP, van den Bent MJ, Weller M, Fisher B, Taphoorn MJ, Belanger K, Brandes AA, Marosi C, Bogdahn U, Curschmann J, Janzer RC, Ludwin SK, Gorlia T, Allgeier A, Lacombe D, Cairncross JG, Eisenhauer E and Mirimanoff RO (2005) Radiotherapy plus concomitant and adjuvant temozolomide for glioblastoma. *N Engl J Med* **352**:987-96.

Tontonoz P, Singer S, Forman BM, Sarraf P, Fletcher JA, Fletcher CD, Brun RP, Mueller E, Altiok S, Oppenheim H, Evans RM and Spiegelman BM (1997) Terminal differentiation of human liposarcoma cells induced by ligands for peroxisome proliferator-activated receptor gamma and the retinoid X receptor. *Proc Natl Acad Sci U S A* **94**:237-41.

Torp SH (2002) Diagnostic and prognostic role of Ki67 immunostaining in human astrocytomas using four different antibodies. *Clin Neuropathol* **21**:252-7.

Vitellaro-Zuccarello L, Meroni A, Amadeo A and De Biasi S (2001) Chondroitin sulfate proteoglycans in the rat thalamus: expression during postnatal development and correlation with calcium-binding proteins in adults. *Cell Tissue Res* **306**:15-26.

Wang M, Wise SC, Leff T and Su TZ (1999) Troglitazone, an antidiabetic agent, inhibits cholesterol biosynthesis through a mechanism independent of peroxisome proliferator-activated receptor-gamma. *Diabetes* **48**:254-60.

Willson TM, Brown PJ, Sternbach DD and Henke BR (2000) The PPARs: from orphan receptors to drug discovery. *J Med Chem* **43**:527-50.

Zander T, Kraus JA, Grommes C, Schlegel U, Feinstein D, Klockgether T, Landreth G, Koenigsknecht J and Heneka MT (2002) Induction of apoptosis in human and rat glioma by agonists of the nuclear receptor PPARgamma. *J Neurochem* **81**:1052-60.

Footnotes

CG was supported by a grant of the German research council (GR 2018/1-1); US and MTH were supported by a grant from the German Cancer research council (10-1795). The work was also supported by the Blanchette Hoker Rockefeller foundation.

Conflict of interest: Gary E. Landreth has received financial support for research projects on anti-inflammatory actions of PPARγ agonists by GlaxoSmithKline. Case Western Reserve University holds a US patent on the use of PPARγ agonists in inflammatory indications in the neryous system. The intellectual property and research support do not relate to the anti-neoplastic actions of the drugs.

Molecular Pharmacology Fast Forward. Published on August 3, 2006 as DOI: 10.1124/mol.106.022194
This article has not been copyedited and formatted. The final version may differ from this version.

Figure Legends

Figure 1: **Pioglitazone reduced cellular viability of rat and human glioma cells and proliferation *in vitro*.** Viability of rat C6 glioma cells (A), human U87 and A172 glioma cells (B) or primary astrocytes (C) at 1, 3, 5, 7 days incubated with the PPARγ agonist pioglitazone (pio) (1, 10, 30μM for C6 and primary astrocytes; 30μM for U87 and A172) was assessed using the MTT-assay. Asterisks indicate significant level in student-T-test: ***p<0.0001 (n=10). Cellular viability of human glioma cells A172 after transfection with vector control, two different PPARγ-cDNA's and PPARγ mutant-cDNA (E499Q) after 5 days of pio treatment (D) was assessed by MTT-assay. Data are expressed as percentage viable cells relative to untreated control cultures. Experiments were performed in triplicate and repeated three times. Asterisks indicate significant level in student-T-test: *p<0.05 (n=10), **p<0.005 (n=10).

Figure 2: **Intracerebral and oral administration of pioglitazone significantly reduced tumor growth in the rat glioma model.** C6 glioma cells were injected in rat striata and treated with pio (20 μM) or vehicle (DMSO) via an osmotic pump over 3 days (n=5/group), 6 days (n=5/group), 9 days (n=5/group), 14 days (n=5/group), and 21 days (n=6/group). Pio-treated animals showed significantly smaller tumor volumes (B, D, E, F) compared to untreated animals (A, C, E, F). A, B shows coronal section of a representative part of the tumor. C, D shows a higher magnification of the striatum at the tumor/brain tissue border. A, C: Striatum of a vehicle-treated animal at 21 days, HE-staining, A: Bar: 1mm; C: Bar: 100μm. B, D: Striatum of a pio-treated animal at 21 days, HE-staining, B: Bar: 1mm; D: Bar: 100μm. E: Representation of tumor area in treated (pio) and untreated (vehicle) animals at 21 days. The schematic shows coronary brain

Molecular Pharmacology Fast Forward. Published on August 3, 2006 as DOI: 10.1124/mol.106.022194
This article has not been copyedited and formatted. The final version may differ from this version.

slices with black color representing tumor tissue and white color representing normal brain tissue. The graph shows tumor area per slide level. F: Tumor volumes in cm^3 of pio-treated animals compared to vehicle-treated animals. Data are presented as mean ± SE of five animals per group (3d, 6d, 9d, 14d) or six animals per group (21d). Asterisks indicate significant level in student-T-test: ***p<0.001 (n=5), **p<0.005 (n=5 or n=6). G: After 21 days of intracerebral pio treatment, tumor volumes of the C6 glioma model are reduced by 83% compared to vehicle treated animals. H: In the intracerebral treated group the tumor volumes are reduced by 76.9%. Data are presented as mean ± SE of six animals per group. Asterisks indicate significant level in student-T-test: *p<0.05, **p<0.001 (n=6).

Figure 3: **Pioglitazone treatment induced Bax- and cleaved caspase-3-upregulation *in vivo.*** A: Bax and cleaved caspase-3 expression in whole-hemisphere lysates of C6 rat glioma animals and control at 3, 6, 9, and 14 days of treatment. Vehicle: vehicle-treated animals; Pio: pio-treated animals. Erk2 served as a loading control. B, C: Bax and cleaved caspase-3 expression at 6 days in 4 (vehicle) and 5 (pio) different animals. D, E: Densitometric analysis of Bax or cleaved caspase-3 levels at 3, 6, 9, 14 days: Data are presented as mean ± SE of 3 different western blots. Black bars: vehicle treatment, gray bars: pio treatment. Asterisks indicate significant level in student-T-test: *p≤0.03 (n=3) **p≤0.002 (n=3), ***p≤0.001.

Figure 4: **Pioglitazone induced apoptosis and reduced proliferation.** Cleaved caspase-3 expression and TUNEL expression in the tumors of C6 rat glioma model animals with and without treatment at day 9 (n=5). DAPI counter staining to determine number of tumor cells. Bar: 100 µm. Percentage of cleaved caspase-3 positive tumor

Molecular Pharmacology Fast Forward. Published on August 3, 2006 as DOI: 10.1124/mol.106.022194
This article has not been copyedited and formatted. The final version may differ from this version.

cells at 6, 9, and 14 days and TUNEL positive tumor cells at 9 days. Data are presented as mean ± SE of the 5 animals per group. Black bars: vehicle treatment, gray bars: pio treatment. Asterisks indicate significant level in student-T-test: **p<0.008 (n=5).

Ki-67 expression and BrdU incorporation in the tumors of C6 rat glioma model animals with and without treatment at day 14 (n=5). DAPI counter staining to determine number of tumor cells. Bar: 100 µm. Percentage of Ki-67 positive tumor cells (proliferation-index) at 9, 14, and 21 days and percentage of BrdU positive tumor cells at 14 days. Data are presented as mean ± SE of the 5 animals per group. Black bars: vehicle treatment, gray bars: pio treatment. Asterisks indicate significant level in student-T-test: *p=0.0114 (n=5); **p≤0.006 (n=5 or n=5).

Figure 5: **Pioglitazone reduces MMP9 protein levels and induces the astrocytic redifferentiation marker CS-56 *in vivo.*** MMP-9 and CS-56 expression. A: MMP-9 expression in whole-hemisphere lysates of C6 rat glioma model animals using a goat-anti-MMP-9-antibody. Vehicle: vehicle-treated animals (n=3); Pio: pio-treated animals (n=3). To ensure equal loading of proteins, each membrane was stripped and reprobed with a rabbit anti-Erk2-antibody. B: Densitometry: Data are presented as mean ± SE of the seven animals per group. Black bars: vehicle treatment, gray bars: pio treatment. Asterisks indicate significant level in student-T-test: ***p=0.0009 (n=3). C: CS-56 (red)/MMP-9 (green) expression at the tumor margin in brain tissue of vehicle- (two left rows) and pio- (two right rows) treated animals. Bars: 100 µm. DAPI-staining served as counterstaining. D: CS-56 expression in whole-hemisphere lysates of C6 rat glioma model animals using a mouse-anti-CS-56-antibody. Vehicle: vehicle-treated animals (n=3); Pio: pio-treated animals. To ensure equal loading of proteins, each membrane

Molecular Pharmacology Fast Forward. Published on August 3, 2006 as DOI: 10.1124/mol.106.022194
This article has not been copyedited and formatted. The final version may differ from this version.

was stripped and reprobed with a rabbit anti-Erk2-antibody. E: Densitometry: Data are presented as mean ± SE of the seven animals per group. Black bars: vehicle treatment, gray bars: pio treatment. Asterisks indicate significant level in student-T-test: **p=0.0012 (n=3).

Figure 1

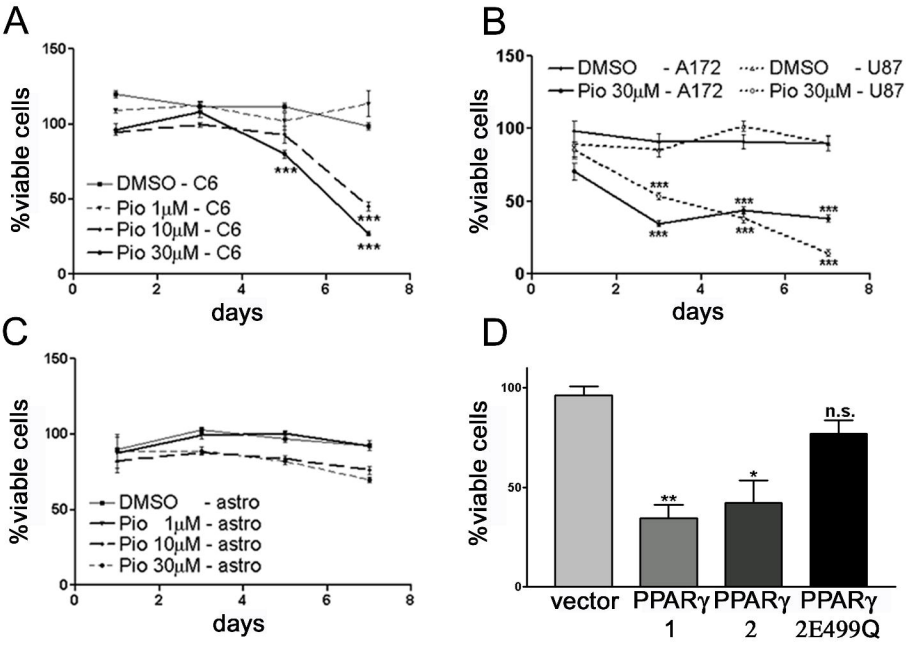
A
%viable cells
days
DMSO - C6
Pio 1μM - C6
Pio 10μM - C6
Pio 30μM - C6
B
%viable cells
days
DMSO - A172
Pio 30μM - A172
DMSO - U87
Pio 30μM - U87
C
%viable cells
days
DMSO - astro
Pio 1μM - astro
Pio 10μM - astro
Pio 30μM - astro
D
%viable cells
n.s.
vector
PPARγ 1
PPARγ 2
PPARγ 2E499Q

Figure 2

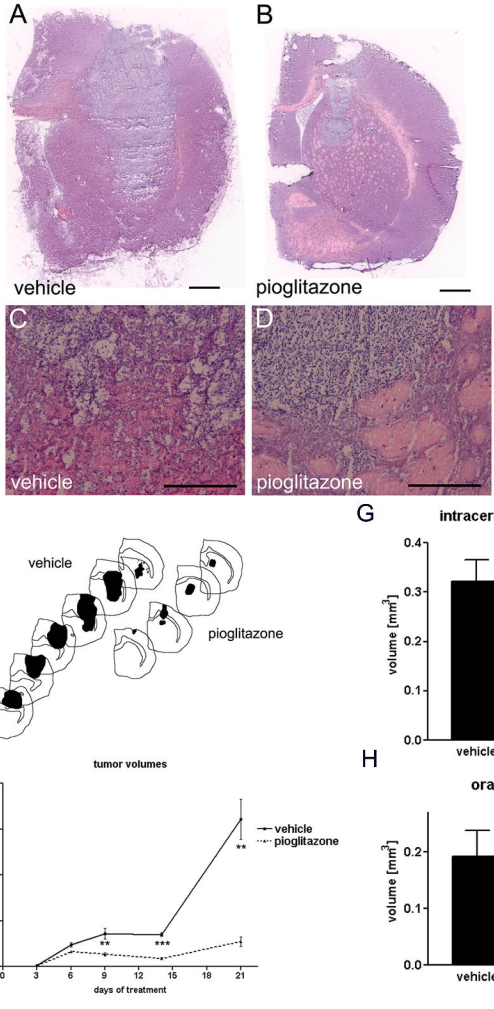
A
B
vehicle
pioglitazone
C
D
vehicle
pioglitazone
E
vehicle
pioglitazone
G
intracerebral therapy
volume [mm3]
0.4
0.3
0.2
0.1
0.0
**
vehicle
Pioglitazone
F
tumor volumes
volume [cm3]
0.4
0.3
0.2
0.1
0.0
vehicle
pioglitazone
**
**
***
**
0
3
6
9
12
15
18
21
days of treatment
H
oral therapy
volume [mm3]
0.2
0.1
0.0
*
vehicle
Pioglitazone

Figure 3

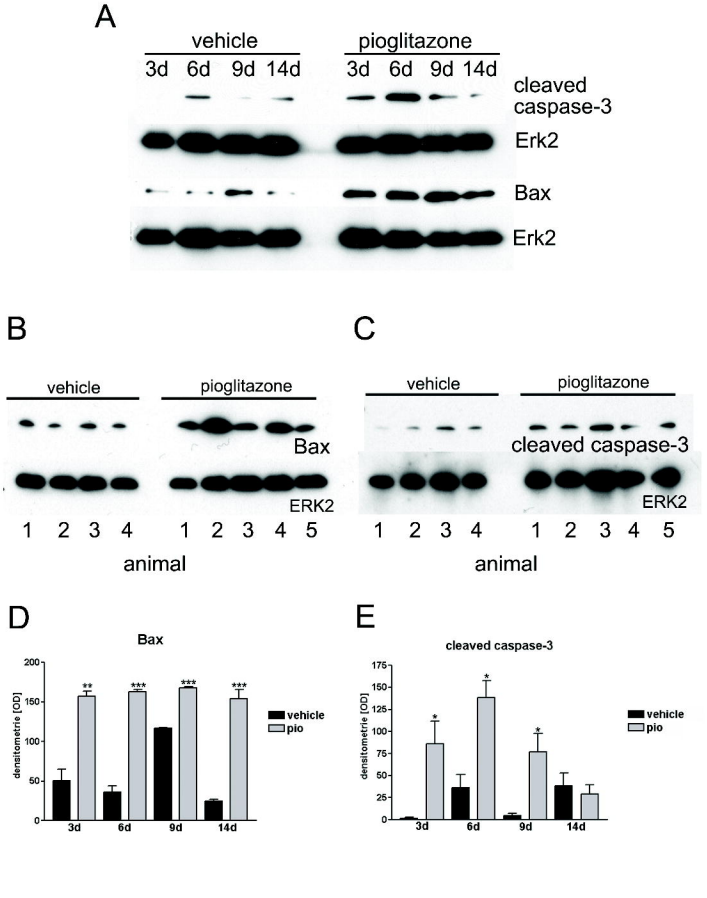
A
vehicle
pioglitazone
3d 6d 9d 14d
3d 6d 9d 14d
cleaved caspase-3
Erk2
Bax
Erk2
B
vehicle
pioglitazone
Bax
ERK2
1 2 3 4 1 2 3 4 5
animal
C
vehicle
pioglitazone
cleaved caspase-3
ERK2
1 2 3 4 1 2 3 4 5
animal
D
Bax
densitometrie [OD]
200
150
100
50
0
**
***
***
***
vehicle
pio
3d 6d 9d 14d
E
cleaved caspase-3
densitometrie [OD]
175
150
125
100
75
50
25
0
*
*
*
vehicle
pio
3d 6d 9d 14d

Figure 4

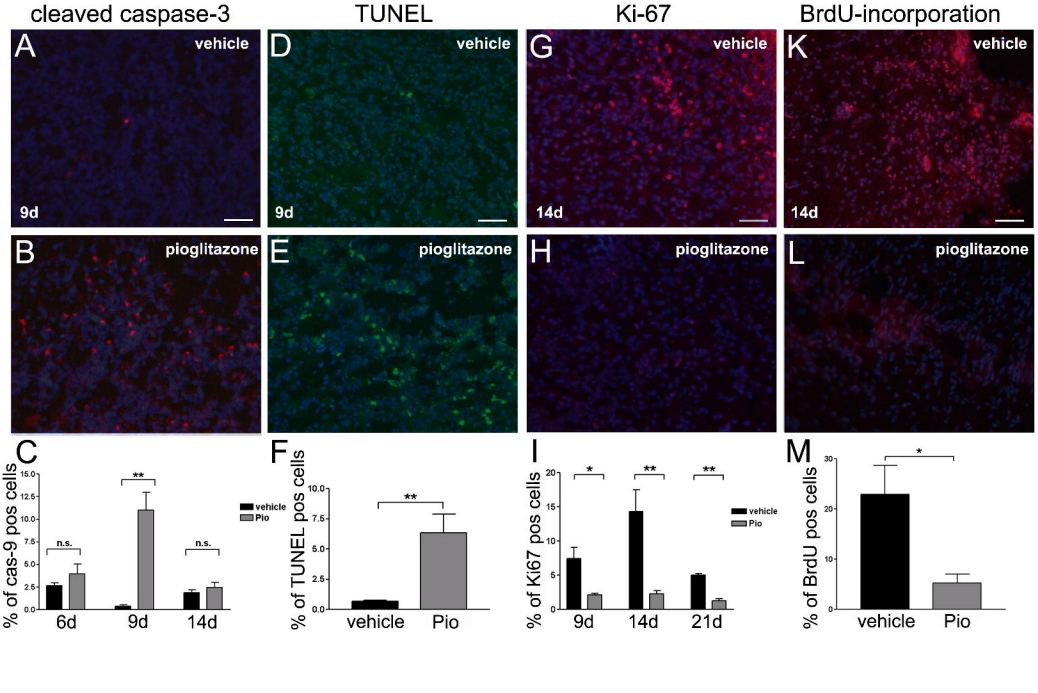
cleaved caspase-3
TUNEL
Ki-67
BrdU-incorporation
A
vehicle
9d
D
vehicle
9d
G
vehicle
14d
K
vehicle
14d
B
pioglitazone
E
pioglitazone
H
pioglitazone
L
pioglitazone
C
% of cas-9 pos cells
n.s.
**
n.s.
6d
9d
14d
vehicle
Pio
F
% of TUNEL pos cells
**
vehicle
Pio
I
% of Ki67 pos cells
*
**
**
9d
14d
21d
vehicle
Pio
M
% of BrdU pos cells
*
vehicle
Pio

Figure 5

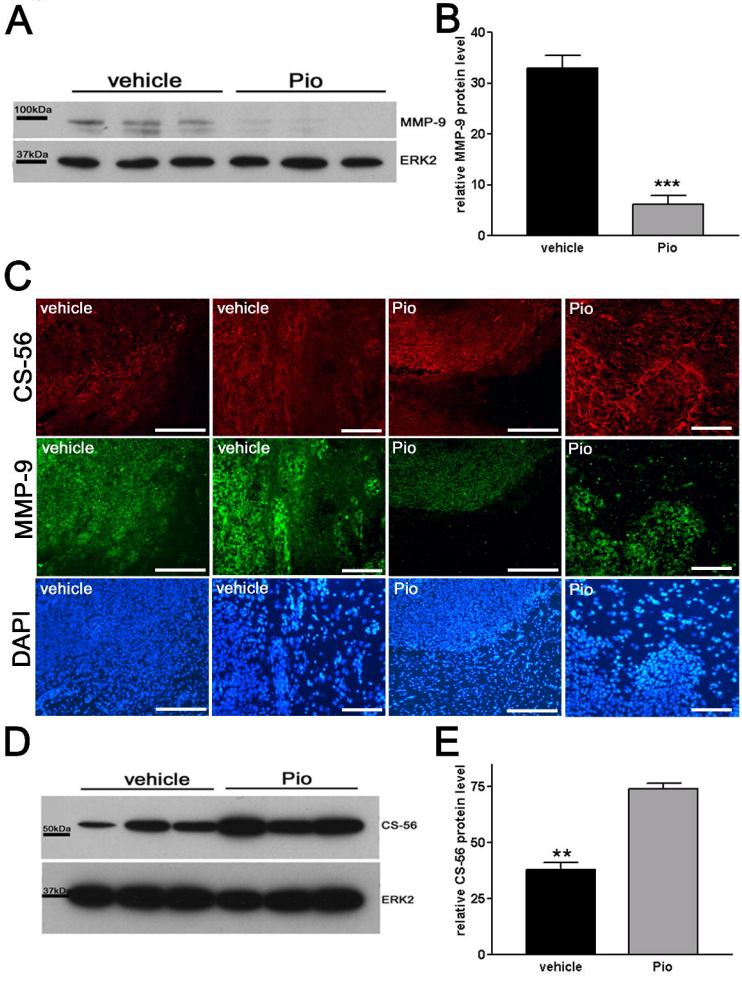
A
vehicle
Pio
100kDa
MMP-9
37kDa
ERK2
B
relative MMP-9 protein level
40
30
20
10
0
***
vehicle
Pio
C
CS-56
MMP-9
DAPI
vehicle
vehicle
Pio
Pio
D
vehicle
Pio
50kDa
CS-56
37kDa
ERK2
E
relative CS-56 protein level
75
50
25
0
**
vehicle
Pio